*Journal of Power Sources, 43–44* (1993) 657–665 

# Structural and electrochemical characteristics of a hollandite-type '$Li_xMnO_2$'

Ph. Botkovitz*, Ph. Deniard, M. Tournoux and R. Brec
*I.M.N., 2 rue de la Houssinière, 44072 Nantes Cedex 03 (France)*

**Abstract**

Possible sites for lithium intercalation in prelithiated $\alpha$-$MnO_2$ compounds are studied by electrochemical techniques. Two types of behaviour, corresponding to different lithium localizations in the prelithiated material are evidenced and they give different electrochemical capacities.

## Introduction

For several years, secondary batteries with lithium as anode and nonaqueous electrolyte have been the subject of intense and important research activities, because of the great need for efficient energy storage systems.

Within this application frame, '$MnO_2$' has been the subject of many experiments. It is used in its $\gamma$-form in primary batteries, but it appeared that it could not be used in this allotropic form in Li rechargeable systems, because of irreversible structural modifications induced by Li reaction [1, 2]. However, remarkable progresses have been achieved these last few years in the developing of secondary $MnO_2$/Li batteries, using spinel-type structures $\alpha$, $\gamma/\beta$, $\beta$ or $\delta$-$MnO_2$ varieties. The $\alpha$-variety has been subject to very few studies although its behaviour appeared promising [3–6]. $\alpha$-$MnO_2$ belongs to the hollandite type. It is built up from $MnX_6$ octahedra (X = O or OH). The $MnX_6$ octahedra share edges and corners to form a double chain along the $c$-axis (Fig. 1). Trials of cycling on an $\alpha$-$MnO_2$ lithiated phase made by Lecerf *et al.* [7] yielded promising data, with energy densities around 490 W h/kg per cycle over a hundred cycles. Our studies have been carried out in collaboration with Lecerf, Alcatel Alsthom Recherche and SAFT. In this paper, we report the characterization and electrochemical behaviour of prelithiated $\alpha$-$MnO_2$ [7] and we discuss the $Li^+$ localization in the hollandite network before and after cycling.

## Experimental

### *Sample preparation*

Prelithiated $\alpha$-$MnO_2$ was obtained by solid-phase reaction between $NH_4Mn_8O_{16}$ and $LiOH \cdot H_2O$ at 300 to 400 °C. $NH_4Mn_8O_{16}$ itself was synthesized by precipitation from a reaction between a $MnSO_4$ solution and $(NH_4)_2S_2O_8$ as an oxidizing agent.

*Author to whom correspondence should be addressed.

0378-7753/93/$6.00 

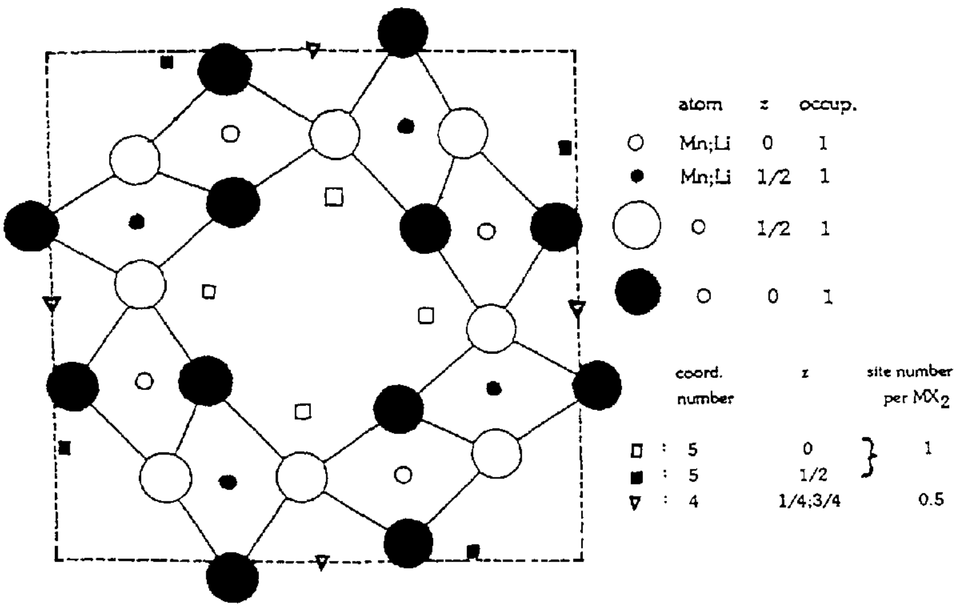


Fig. 1. Lithiated $\alpha$-$MnO_2$ unit cell projection along [001] direction. (●), (○), (▽), (□) and (■) are possible sites for lithium (respectively octahedral (●, ○), tetragonal (▽) and five coordination sites (□, ■)).

Four samples (labelled a, b, c and d) obtained under different synthesis conditions have been studied. These pristine materials have been characterized by X-ray diffraction, IR spectroscopy and chemical analyses. X-ray diffraction was performed using an INEL CPS 120 detector (Cu $K\alpha_1$ radiation). A Fourier-transform infrared spectrometer (Nicolet 20 SXC) as well as quantitative analyses based on the Kjeldahl method were used to evaluate the remaining $NH_4^+$ ions concentration in the compound. Chemical analysis of $Li^+$ ions were obtained by atomic absorption (Philips PU 9000), whereas both atomic absorption and complexometry allowed us to determine the manganese concentration. Manganese oxidation state was achieved by back titration technique: after dissolution in hot acidic medium ($H_3PO_4$/$H_2SO_4$), with a Mohr salt excess and under a nitrogen flow, the remaining $Fe^{2+}$ ions were titrated by a $K_2Cr_2O_7$ solution. For the proton analysis, the samples were heated at about 1100 °C under oxygen flow. Resulting $H_2O$ was transformed into $CO_2+H_2$ by reaction with active carbon at 1120 °C, then a coulombic method was used for the $CO_2$ titration.

*Electrochemical tests*

Li/[1 M $LiCF_3SO_3$ in PC/EC/DME (1/1/2)/'$\alpha$-$MnO_2$' electrochemical button cells were used for all experiments. '$\alpha$-$MnO_2$' cathodes consisted of a mass of 80% prelithiated $\alpha$-$MnO_2$, 15% carbon and 5% Teflon binder. Cycling from 2 to 3.8 V were driven by a Macpile system [8] under constant current at a $C/10$ rate. A thirty minute relaxation followed each charge or discharge. Thermodynamic tests using galvanostatic technique were performed with the same apparatus: a 50 $\mu$A pulse of 30 min was applied to the cell before a potential relaxation ending with a $dV/dT<10$ mV/h condition. Galvanostatic tests were preferred to voltammetry experiments in order to be consistent with previous SAFT obtained data. These two methods led to the same results as it is possible to convert galvanostatic data into incremental capacity ones ($dQ/dV=f(V)$). In the case of incremental capacity, each peak corresponds to a plateau in conventional $V=f(Q)$ curve, where $Q$ is expressed in F per mole of cathodic material. Each step of intercalation induced a peak whose area is proportional to intercalated Li amount at this particular energy.

## Results and discussion

Prelithiated $\alpha$-$MnO_2$ compounds do not present a long range order: X-ray diagrams give wide peaks with a very poor signal-to-noise ratio, irrespective of the radiation used (Cu $K\alpha_1$, Fe $K\alpha_1$, Mo $K\alpha_1$). The hollandite-type structure seems however to be retained in prelithiated $\alpha$-$MnO_2$ [9]. Table 1 gives the X-ray pattern of $NH_4Mn_8O_{16}$ ($a=9.865(3)$ Å; $c=2.849(1)$ Å, before and after lithiation. The lithiation maintains the $c$ parameter whereas the $a$ parameter changes from 9.865(3) to 9.93(4) Å.

TABLE 1

X-ray powder data[a]

| $h\ k\ l$ | $d_{calc.}$ | $d_{obs.}$ | Relative intensity | Fwhm (°) |
|---|---|---|---|---|
| *(a) $NH_4Mn_8O_{16}$ ($a=9.865(3)$ Å, $c=2.849(1)$ Å)* | | | | |
| 1 1 0 | 6.97 | 6.99 | 100 | 0.45 |
| 2 0 0 | 4.931 | 4.932 | 89 | 0.48 |
| 3 1 0 | 3.118 | 3.116 | 66 | 0.54 |
| 4 0 0 | 2.465 | 2.471 | 14 | 0.39 |
| 2 1 1 | 2.393 | 2.394 | 85 | 0.34 |
| 3 3 0 | 2.324 | 2.324 | 14 | 0.36 |
| 3 0 1 | 2.153 | 2.152 | 24 | 0.32 |
| 4 1 1 | 1.8319 | 1.8321 | 63 | 0.57 |
| 6 0 0 | 1.6438 | 1.6449 | 42 | 0.97 |
| 5 2 1 | 1.5406 | 1.5395 | 76 | 0.71 |
| 0 0 2 | 1.4244 | 1.4253 | 21 | 0.55 |
| 5 4 1 | 1.3549 | 1.3554 | 27 | 0.54 |
| 3 1 2 | 1.2957 | 1.2958 | 60 | 1.51 |
| *(b) $\alpha$-$MnO_2$ lithiated compounds ($a=9.93(4)$ Å, $c=2.840(4)$ Å)* | | | | |
| 1 1 0 | 7.02 | 7.00 | 95 | 0.81 |
| 2 0 0 | 4.964 | 4.233 | 70 | 0.74 |
| 3 1 0 | 3.139 | 3.158 | 74 | 1.10 |
| 2 1 1 | 2.392 | 2.395 | 100 | 0.58 |
| 3 0 1 | 2.155 | 2.142 | 42 | 1.36 |
| 4 1 1 | 1.8365 | 1.8383 | 35 | 0.72 |
| 5 2 1 | 1.5463 | 1.5464 | 53 | 1.09 |
| 0 0 2 | 1.4198 | 1.4210 | 23 | 0.50 |
| 2 0 2 | 1.3651 | 1.3650 | 48 | 1.02 |

[a]The refinements are performed in tetragonal symmetry.

Infrared spectroscopy has given evidence of impurities such as $Li_2MnO_3$, $Mn(NO_3)_2$, $Li_2CO_3$ and $SO_4^{2-}$ anions. Their respective amounts have been determined by X-ray diffraction and analysis of the elements N, C and S. All these impurities correspond to about 10 wt.% of the material and are electrochemically inactive. The hollandite-phase formulation $Li_x[Mn_{1-y}Li_y](O_{2-z}OH_z)\cdot(H_2O)_t$ (referred to as '$\alpha$-$Li_xMnO_2$') has been established from experimental parameters: wt.% Mn, wt.% Li and manganese oxidation state, after correction to take into account the impurities.

The analyses of the samples a, b, c and d led to chemical formulations very close to each other excepted for impurities. The average formulation is:

$$Li_{0.3}[(Mn^{3.9+})_{0.92}Li_{0.08}](O_{1.92}OH_{0.08})\cdot(H_2O)_{0.06} \tag{1}$$

Lithium ions localized in octahedral sites substitute manganese to compensate the charge deficiency. The manganese ions have a 3.9 mean oxidation state that corresponds to a $Mn^{III}$:$Mn^{IV}$ ratio of 0.11. Lithium resulting from chemical reaction with $NH_4Mn_8O_{16}$ to form prelithiated '$\alpha$-$Li_xMnO_2$' will be mentioned below as 'chemical lithium'.

*Sites available in the structure for chemical lithium*

Lithium localization by X-ray diffraction is not possible, due in part to the poor diagram quality. Nuclear magnetic resonance (NMR) Magic Angle Spinning experiment technique failed also, because of $Mn^{3+}$ and $Mn^{4+}$ paramagnetism. All the possible sites for Li suggested below result from geometrical considerations based on the structure of the pristine material supposed to present an ideal hollandite structure. Three favourable sites can be found (Fig. 1): octahedral sites in substitution of manganese, tetrahedral sites in the [1×1] tunnels and five coordination sites in the [2×2] tunnels borders. Although eight coordinated central sites correspond to geometrical properties convenient for Li, their coordination is too high and the size too big for Li. 0.08 octahedral sites are occupied by $Li^+$. The 0.3 remaining Li can be localized in the 0.5 tetrahedral or five coordination sites (the site counting corresponds to one '$MnO_2$').

*Electrochemical experiments*

*Thermodynamic tests condition*

The four samples led to Li intercalation spanning from 0.66 to 0.70 Li. As mentioned above, only 0.5 tetrahedral sites are available per '$MnO_2$' formulation. This implies that Li intercalation partially concerns large tunnels and, on the basis of a steric aspect, Li ions intercalate probably only in these last sites.

*Constant current cycling*

$V=f(Q)$ cycling curves, where $Q$ is the Faraday number per '$MnO_2$' formulation are presented on Fig. 2. Positive values of $\Delta Q$ correspond to intercalated Li. From the first cycle, $Q_{min}$ ($Q$ at the end of charge) is negative and decreases linearly as cycling proceeds (Fig. 3). This means that the number of charges extracted from the cathode is greater than the ones introduced during discharge. Two possibilities may correspond to such a behaviour: electrolyte oxidation or irreversible deintercalation of 'chemical lithium'. Electrochemical tests on electrolyte show sizeable oxidation current above 3 V.

From sample b in Fig. 4, the only compound for which the number of recorded cycles is large enough, one can clearly notice that the slope of the curve changes near the 150th cycle (it goes from −0.00233 to −0.00156). Considering that electrolyte

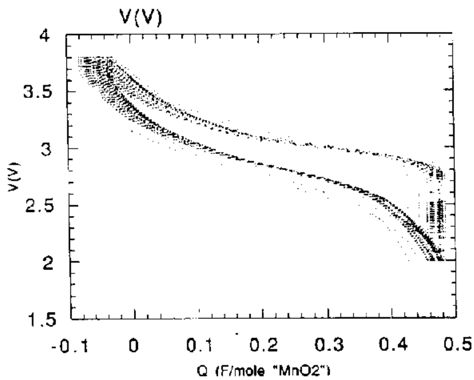


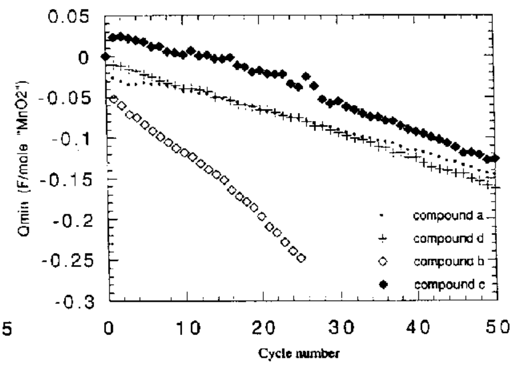


Fig. 2. Typical cycling curves $V=f(Q)$ for '$\alpha$-$Li_xMnO_2$' phases. Example is given for compound a.

Fig. 3. $Q_{min}$ vs. cycle number for compounds a, b, c and d.

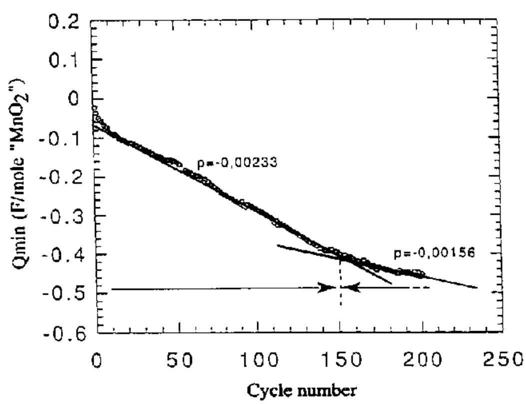


Fig. 4. $Q_{min}$ vs. cycle number for compound b. Notice the flattening of slope at the 150th cycle.

oxidation is not different before and after the 150th cycle, the non zero slope after the 150th cycle must correspond to the electrolyte oxidation which participates to the variation of $Q_{min}$ in the ratio 156:233. The first part of the slope must be due to both electrolyte oxidation and 'chemical lithium' extracted from the material. This Li extraction contribution is (0.00233–0.00156):0.00233. One can then calculate that 0.13 'chemical lithium' are extracted from the initial 0.3 Li available (it is assumed that the 0.08 Li ions located within the frame have a much lower mobility and are not removed), which corresponds actually, within errors, to the amount of $Mn^{3+}$ to be oxidized into $Mn^{4+}$.

A careful analysis of the incremental capacity curves during discharge (Fig. 5) allows to detect the occurrence of an initial peak at 2.7 V and a shoulder between 3.7 and 3.1 V. On cycling, a peak at 3 V appears. Then the 2.7 and 3 V peaks experience a parallel shift in potential. At the same time, the peak initially at 3 V decreases its intensity, whereas the peak initially at 2.7 V disappears after the 18th cycle. This is the proof of an important structural alteration during the first cycles.

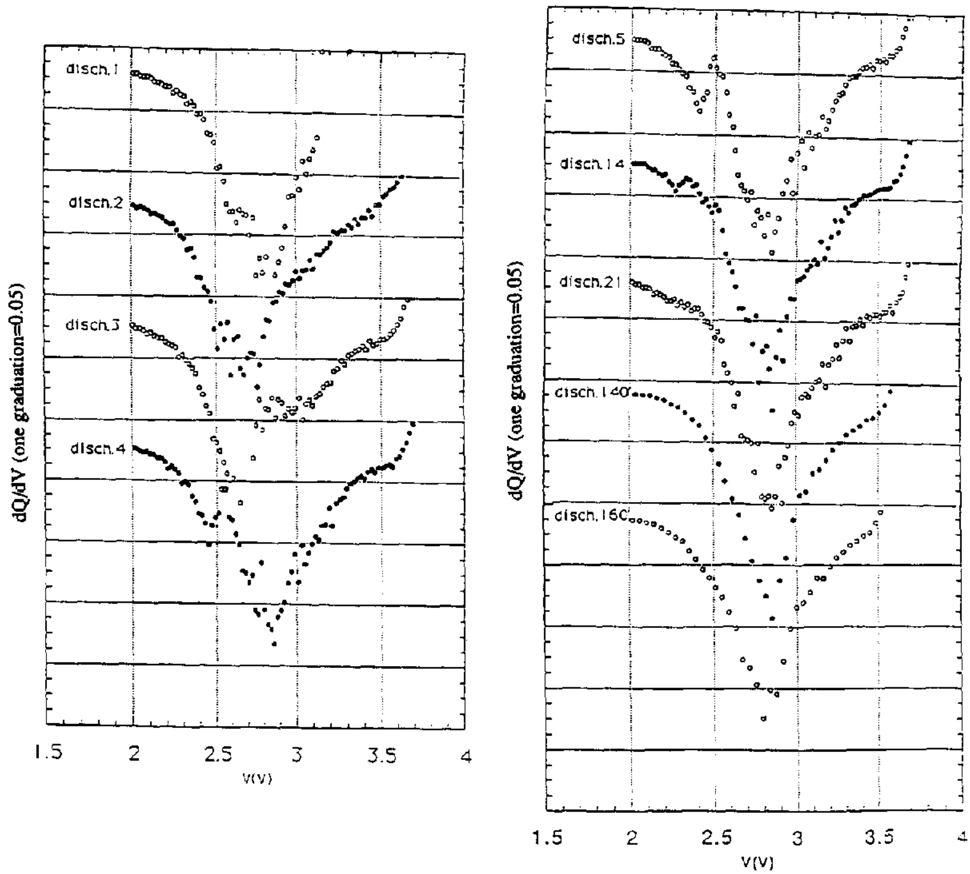


Fig. 5. Incremental capacity evolution curves with cycling for compound b.

The analysis of the potential evolution may be performed as follows: the shoulder between 3.7 and 3.1 V is well apparent during the first cycles and corresponds to an insertion amount of 0.12 Li per ' $MnO_2$' unit. It decreases with cycling to disappear at the 150th cycle, which results in the vanishing of the corresponding shoulder on the incremental capacity curves. The disappearing of these 0.12 insertion sites may be correlated to the extraction of the 0.13 'chemical lithium'. It may be thought that the insertion of the 0.12 Li takes place in the vicinity of these initial 'chemical lithium' ions which presence within the structure would imply the same number of sites with a characteristic energy (the shoulder between 3.7 and 3.1 V). Assuming, reasonably, that the electrochemical insertion takes place within the large tunnels (it is to be recalled that up to 0.7 Li can be intercalated under equilibrium conditions, i.e., more than the number of availables sites if one excludes the large cubic voids), the 0.13 removable 'chemical lithium' ions must be found in there in privileged sites, which differentiates them from the inserted $Li^+$. The remaining 0.17 $Li^+$ cannot be found then in the large tunnels, since they should be detected on the incremental capacity curves. They can only be found in the skeleton *Td* sites.

Incremental capacity evolution as a function of cycling, is the same for the compounds a and b whereas it has a different behaviour for c and d (Fig. 6) for which the 3.1 to 3.7 V shoulder has disappeared. Such a difference between the two groups of samples is also found in cycling capacities under constant current (Fig. 7). They concern 0.55 F per '$MnO_2$' for compounds a and b whereas only 0.45 F is found for samples c and d. Thus, it is obvious to correlate this difference of capacity to the 3.1 to 3.7 V shoulder (Fig. 8). As this shoulder depends on extractable 'chemical lithium', one can easily understand that it has a contribution when it goes out of the structure. As this shoulder depends on extractable 'chemical lithium', we can conclude that its presence is necessary to a better cycling capacity.

It results from this discussion that the complete new formulation to be put forward for the lithiated hollandites under study is:

$$Li_{0.13}(\mathit{Tun})Li_{0.17}(\mathit{Td})[Li_{0.08}Mn_{0.92}]\mathit{Oh}[O_{1.92}(OH)_{0.08}](H_2O)_{0.06}(SO_4)_{0.025} \quad (2)$$

for compounds a and b and:

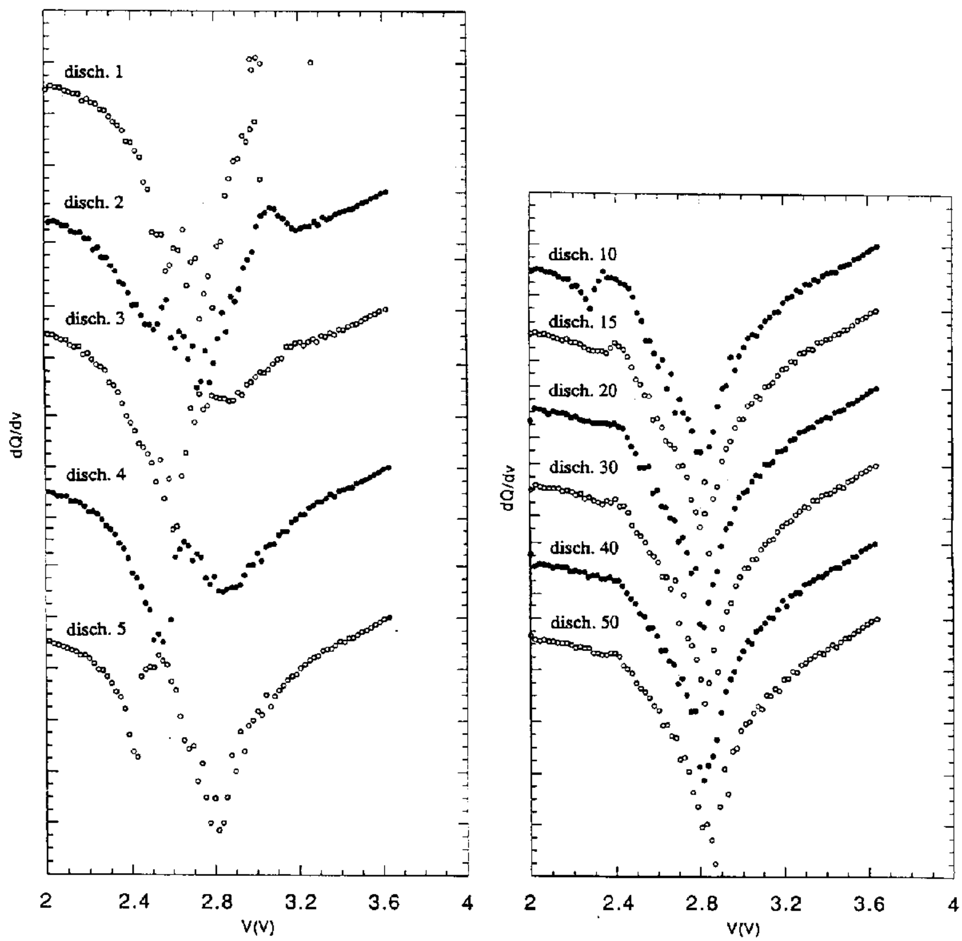


Fig. 6. Incremental capacity evolution curves with cycling for compounds c and d.

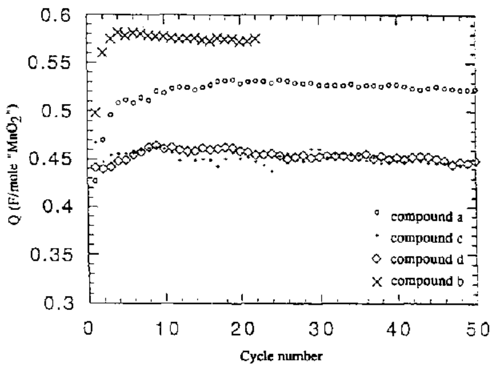


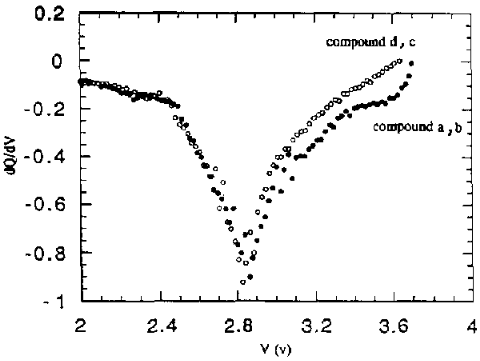


Fig. 7. Capacity vs. cycle number for compounds a, b, c and d.

Fig. 8. Incremental capacity for compounds c, d and a, b after the 20th cycle (the system is then stabilized). Differences in peak areas (area is proportional to the capacity) is located between 3.1 and 3.7 V.

$$Li_{0.30}(Td)[Li_{0.08}Mn_{0.92}]Oh[O_{1.92}(OH)_{0.08}](H_2O)_{0.06}(SO_4)_{0.025} \quad (3)$$

for compounds c and d.

## Conclusion

'$\alpha$-$Li_xMnO_2$' compounds resulting from lithiation of $NH_4Mn_8O_{16}$ can thus be separated in two groups with different electrochemical capacities. The first one gives about 0.45 F per '$MnO_2$' when the second leads to capacities reaching 0.55 F per formulation. These two types of behaviour can be correlated with the presence, within the structure large tunnels, of 'chemical lithium' which is necessary to obtain a good cycling capacity. All these assumptions have to be verified by different techniques namely neutron diffraction experiments. The remaining point will then be understood which factors of the synthesis govern the possibility for 'chemical lithium' to be found in the large tunnels and how this one interacts on the cycling capacity. The comprehension of these factors should allow to obtain enhanced capacities for '$\alpha$-$Li_xMnO_2$'.

## Acknowledgements

We want to thank Alcatel Alsthom Recherche and SAFT, for the financial support of this work.

## References

1 G. Pistoia, *J. Electrochem. Soc.*, *129* (1982) 1861.
2 J. Desilvestro and O. Haas, *J. Electrochem. Soc.*, *137* (1990) 5c.
3 H. Ikeda, in J. P. Gabano (ed.), *Lithium Batteries*, Academic Press, London, 1983, p. 169.
4 N. Furukawa, T. Saito, K. Teraji, I. Nakane and T. Nohma, *Ext. Abstr., The Electrochemical Society Meet., 1987, Honolulu, HI, USA*, Vol. 87-2, 1987, p. 94.

5 T. Ohzuku, M. Kitagawa, K. Sawai and T. Hirai, *J. Electrochem. Soc., 138* (1991) 360.
6 M. H. Rossouw, D. C. Liles, M. Tackeray, W. David and S. Hull, *Mater. Res. Bull., 27* (1992) 221.
7 A. Lecerf, F. Lubin and M. Brussely, *SAFT US Patent No. 4 975 346* (accepted Dec. 4, 1990).
8 C. Mouget and Y. Chabre, *Multichannel potentiostat and galvanostat,* Macpile, Licensed from CNRS and UJF Grenoble to BIO, Logic Co., 1 Av. de L'Europe, F-38640 Claix.
9 F. Lubin, *Thesis,* University of Rennes, 1991.